Universal Casimir Interaction between Two Dielectric Spheres in Salted Water

Tanja Schoger[,1] Benjamin Spreng[,2] Gert-Ludwig Ingold[,1,*]
Paulo A. Maia Neto[,3,†] and Serge Reynaud[4,‡]

[1]*Universität Augsburg, Institut für Physik, 86135 Augsburg, Germany*
[2]*Department of Electrical and Computer Engineering, University of California, Davis, California 95616, USA*
[3]*Instituto de Física, Universidade Federal do Rio de Janeiro, Rio de Janeiro, Rio de Janeiro 21941-972, Brazil*
[4]*Laboratoire Kastler Brossel, Sorbonne Université, CNRS, ENS-PSL, Collège de France, Campus Jussieu, 75005 Paris, France*

We study the Casimir interaction between two dielectric spheres immersed in a salted solution at distances larger than the Debye screening length. The long distance behavior is dominated by the nonscreened interaction due to low-frequency transverse magnetic thermal fluctuations. It shows universality properties in its dependence on geometric dimensions and independence of dielectric functions of the particles, with these properties related to approximate conformal invariance. The universal interaction overtakes nonuniversal contributions at distances of the order of or larger than 0.1 μm, with a magnitude of the order of the thermal scale $k_B T$ such as to make it important for the modeling of colloids and biological interfaces.

The electromagnetic Casimir effect [1–3] and the so-called critical Casimir effect [4–8] are two examples of long-range forces appearing when fluctuations are confined within walls [9]. The former is often considered as associated to quantum field fluctuations and the latter to classical thermal fluctuations in matter. A problem sharing properties with both of them corresponds to the high-temperature limit of the electromagnetic Casimir interaction between bodies separated by a medium.

The case of two metallic spheres described by a Drude conductivity model in vacuum has been shown to lead to a universal expression in the limit of high temperatures or, equivalently, of large distances, with the free energy not depending on the details of the electromagnetic response of the involved material [10,11]. At room temperature $T \sim 300$ K, this universal thermal Casimir contribution overtakes the nonuniversal terms at large distances [12] of the order of the thermal wavelength $\hbar c / k_B T \sim 7.6$ μm, making its experimental detection challenging as the magnitude of the force is decreasing as a power-law function of the distance [13].

We will consider in this Letter a complementary case with two dielectric particles separated by a conducting electrolyte solution. In this case, there is also a universal classical expression in the limit of high temperatures, with the free energy not depending on the detailed dielectric function of the involved material. The universal thermal contribution now overtakes the sum of nonuniversal terms at a much smaller distance ℓ_T of the order of 0.1 μm for typical materials considered in this context [14,15]. The existence and magnitude of this universal Casimir interaction have recently been confirmed by measurements [16] involving a silica microsphere held by optical tweezers [17] in the vicinity of a larger sphere, with both spheres immersed in salted water.

The high-temperature Casimir interaction between dielectric spheres in a conducting solution is a universal function of the geometry that can be derived exactly with the help of analytical and numerical tools based on the scattering approach [18] by using the plane-wave basis [19]. We present below the universal interaction free energy obtained in this manner and show that it can reach the thermal energy scale $k_B T$, which makes it important for the description of biological interfaces and colloidal solutions [20].

In the following, we study the Casimir interaction between two dielectric spheres immersed in a salted solution at ambient temperature under the assumptions that the distance of closest approach L between the spheres is much larger than the Debye screening length λ_D and larger than the length ℓ_T introduced above. The first assumption implies that electrostatic interactions resulting from surface charges or electric potential fluctuations [21–23] are efficiently screened while the second assumption ensures that the force is dominated by the Matsubara term at zero frequency [24]. Under these assumptions, the main force is due to the Casimir interaction mediated by low-frequency transverse magnetic thermal fluctuations coupled to electric multipoles.

We have calculated numerically the exact free energy for the geometry of two spheres with arbitrary radii by adapting the plane-wave approach introduced in Ref. [19] to our problem. It turns out that the free energy shows universality properties for arbitrary values of geometric

parameters and, in particular, that the interaction does not depend on the dielectric functions of the spheres. We first recall the method for calculating the free energy and then give approximated expressions allowing one to obtain simple estimates for it without having to perform the complete numerical calculation.

The free energy $\mathcal{F}_T$ in the high-temperature limit can be written as the product of an energy scale, the thermal energy $k_B T$, and a dimensionless function f_u depending only on two ratios of the geometric dimensions L, R_1, and R_2:

$$\mathcal{F}_T(L, R_1, R_2) = -k_B T f_u. \qquad (1)$$

The negative sign of $\mathcal{F}_T$ implies attraction between the spheres. As f_u does not depend on T, the entropy is $\mathcal{S} = k_B f_u$ and the free energy is $\mathcal{F}_T = -T\mathcal{S}$, so that the Casimir force is purely entropic in nature here.

The parameter used as a subscript in f_u measures the ratio of radii in an expression symmetric in R_1, R_2:

$$u = \frac{R_1 R_2}{(R_1 + R_2)^2}. \qquad (2)$$

It lies in the range $0 \leq u \leq 1/4$, with $u = 0$ corresponding to a plane-sphere geometry and $u = 1/4$ to two spheres of equal radii. A natural choice for the other parameter could be the dimensionless distance,

$$x = \frac{L}{R_{\text{eff}}}, \qquad (3)$$

where $R_{\text{eff}} = R_1 R_2/(R_1 + R_2)$ is the effective radius of the system of two spheres. We will see however that a better parameter for describing the dependence of f_u on distance is

$$y = \frac{(L + R_1 + R_2)^2 - R_1^2 - R_2^2}{2 R_1 R_2} = 1 + x + u \frac{x^2}{2}. \qquad (4)$$

This geometric quantity y is invariant under conformal transformations generated by isometries and inversion in three-dimensional Euclidean space [25]. It has been known for a long time [26,27] to simplify the expression of the mutual capacitance C_{12} between the two spheres [C_{12} is written in terms of $\varpi = \text{arcosh}(y)$ in Ref. [27], Pt. 1, Sec. 11].

Within the scattering approach, f_u can be written in terms of an operator $\mathcal{M}$ representing the effect on the electromagnetic field of a single round-trip in the cavity formed by the two spheres:

$$f_u = -\frac{\text{Tr}\log(1 - \mathcal{M})}{2} = \sum_{r=1}^{\infty} f_u^{(r)}, \quad f_u^{(r)} \equiv \frac{\text{Tr}\mathcal{M}^r}{2r}. \qquad (5)$$

The contribution $f_u^{(r)}$ corresponds to a given number r of round-trips in the cavity, and f_u is the sum over all numbers of round-trips. The round-trip operator $\mathcal{M}$ is defined as a product of reflection operators $\mathcal{R}_m$ for the spheres $m = 1, 2$ and translation operators $\mathcal{T}_{m'm}$ from a frame aligned on sphere m to the one aligned on m':

$$\mathcal{M} = \mathcal{R}_1 \mathcal{T}_{12} \mathcal{R}_2 \mathcal{T}_{21}. \qquad (6)$$

These operators can be expressed explicitly in the basis of plane waves [28] characterized by the projection $\mathbf{k}$ of the wave vector onto the plane perpendicular to the line joining the two centers of the spheres with the direction of propagation changing at each reflection.

In this basis, the translation operators are diagonal:

$$\langle \mathbf{k}' | \mathcal{T}_{m'm} | \mathbf{k} \rangle = e^{-k(L + R_1 + R_2)} \delta^{(2)}(\mathbf{k}' - \mathbf{k}), \qquad (7)$$

where $k = |\mathbf{k}|$ is the norm of the projected wave vector $\mathbf{k}$. The reflection operators $\mathcal{R}_1$ and $\mathcal{R}_2$ can be derived by following Ref. [29] and in particular its Appendix B where the zero-frequency limit is described. When considering spheres in salted water instead of vacuum as was done in Ref. [29], we need to replace the static dielectric constant $\varepsilon(0)$ by the ratio $\varepsilon_s(0)/\varepsilon_m(0)$ of static dielectric functions of spheres and medium.

Using salted water as the medium has two consequences for our problem. Moving ions efficiently screen longitudinal modes [15], and we can restrict our attention to transverse magnetic modes. Furthermore, in view of the finite static conductivity of the medium, $\varepsilon_m(0)$ is infinite. Hence, as long as the dielectric functions of the spheres remain finite, any detailed dielectric property of the particles disappears from the matrix elements of the reflection operators $\mathcal{R}_1$ and $\mathcal{R}_2$:

$$\langle \mathbf{k}' | \mathcal{R}_m | \mathbf{k} \rangle = -\frac{2\pi R_m}{k'} \sum_{\ell=1}^{\infty} \frac{\ell}{\ell+1} \frac{[2R_m^2 kk'(1+\cos\varphi)]^\ell}{(2\ell)!}, \qquad (8)$$

with φ the angle between the ingoing and outgoing projected wave vectors $\mathbf{k}$ and $\mathbf{k}'$.

Our numerical results for f_u are shown in Figs. 1 and 2 as functions of x and $y - 1$, respectively, for fixed values of u, i.e., fixed ratios of radii. Both plots show a monotonic decrease of free energy from small to large distances L. Their comparison reveals that the dependence of f_u on u seen on Fig. 1 is largely captured on Fig. 2 by using the abscissa $y - 1 = x[1 + (ux/2)]$, which is a stretched version of x with the stretching factor depending on u. The fact that the different curves f_u are better aligned on Fig. 2 will be given an interpretation by the analytical results presented below.

We follow the method of Ref. [30] and express the Casimir free energy in terms of Gaussian-type integrals. The single round-trip expression thus yields
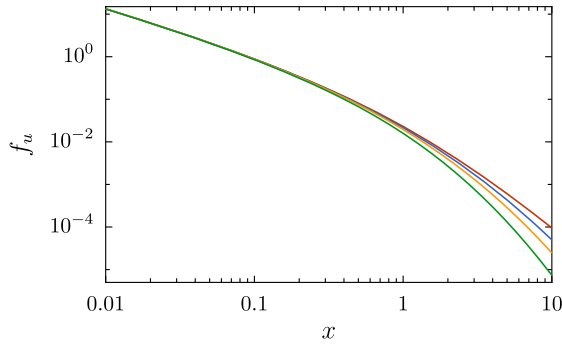
FIG. 1. Reduced free energy f_u for two dielectric spheres in salted water, drawn as a function of $x = L/R_{\text{eff}}$ for different values of $u = 0, 0.04, 0.10, 0.25$ from top to bottom.

$$f_u^{(1)} = \frac{y}{4(y^2-1)} + \frac{z}{12} \log \frac{(y^2-1)z^2}{(yz+\frac{1}{2})^2}$$
$$+ \frac{1}{12\sqrt{z}} \sum_{\eta=\pm} \frac{1}{\alpha_\eta^{3/2}} \log \frac{2y^2 + \alpha_\eta y - 1 + \sqrt{\alpha_\eta z}}{2y^2 + \alpha_\eta y - 1 - \sqrt{\alpha_\eta z}}, \quad (9)$$

where auxiliary variables have been introduced:

$$\alpha_\pm = \frac{1 - 2u \pm \sqrt{1-4u}}{2u}, \qquad z = 2(y-1) + \frac{1}{u}. \quad (10)$$

The function $f_u^{(1)}$ shows basically the same behavior as f_u in Fig. 2. It mainly depends on y, which means that the analytical results nearly obey conformal invariance. But $f_u^{(1)}$ still depends on u through the parameters $\alpha_\pm$, which correspond to the ratios R_1/R_2 and R_2/R_1, and this dependence breaks exact invariance.

The large-distance limit $L \gg R_{\text{eff}}$ is dominated by the single round-trip contribution obtained from the asymptotic expansion of Eq. (9):

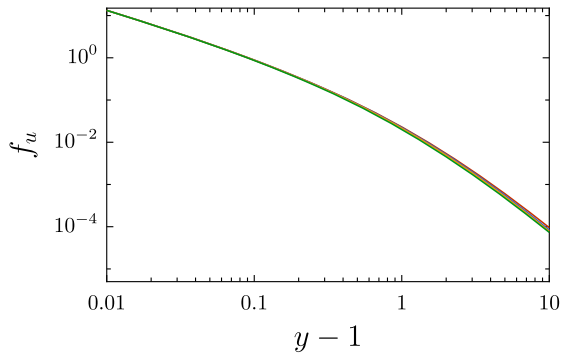$$f_{u=0} \simeq \frac{1}{8y^3}, \qquad f_{u\neq0} \simeq \frac{3}{32y^3} \simeq \frac{3}{4} f_{u=0}. \quad (11)$$

The free energy in the sphere-sphere geometry ($u \neq 0$) is smaller by a factor $3/4$ relative to the plane-sphere geometry ($u = 0$). The ratio $f_u^{(1)}/f_0^{(1)}$ for different values of u is depicted in Fig. 3. For large distances, the curves asymptotically reach the limit $3/4$ if $u \neq 0$. This factor is the main reason for the dependence of f_u on u observed at large values of $y - 1$ in Fig. 2, that is the breaking of exact conformal invariance.

While the asymptotic power-law dependence on y in Eq. (11) is the same for all values of u, this is no longer the case when the free energy is expressed as a function of x. Then, the free energy in the plane-sphere case decreases as x^{-3} while it decays as $(ux^2)^{-3}$ for two spheres, thus explaining why the asymptotics is so different in Fig. 1. In simple words, the asymptotic behaviors (11) explain why using the abscissa $y - 1$ captures most of the distance dependence of the free energy while still weakly breaking exact conformal invariance.

In the short-distance limit $L \ll R_{\text{eff}}$, multiple round-trips need to be accounted for. In this limit, $f_u^{(1)}$ is independent of u and the same holds for multiple round-trips with $f_u^{(r)} \simeq f_u^{(1)}/r^3$. It follows that the sum over r can be written as a simple factor, the Apéry's constant $\zeta(3)$:

$$f_u \simeq \sum_{r=1}^{\infty} \frac{f_u^{(1)}}{r^3} \simeq \frac{\zeta(3)}{8(y-1)}. \quad (12)$$

This result explains why the curves f_u calculated for different values of u tend to become identical when $x \ll 1$ in Fig. 1 and $y - 1 \ll 1$ in Fig. 2. The free energy (12) corresponds to the so-called proximity-force approximation, where the force can be obtained by integrating the pressure calculated between two planes [31] over the range of distances met in the geometry of two spheres. The result (12) also coincides with the short-distance limit of the free energy between Drude spheres in vacuum as the Fresnel reflection amplitudes for the two complementary

FIG. 2. Reduced free energy f_u with the same conventions and scales as on Fig. 1, but for the use of abscissa $y - 1$. The range of abscissas matches that on Fig. 1 for the curve $u = 0$.
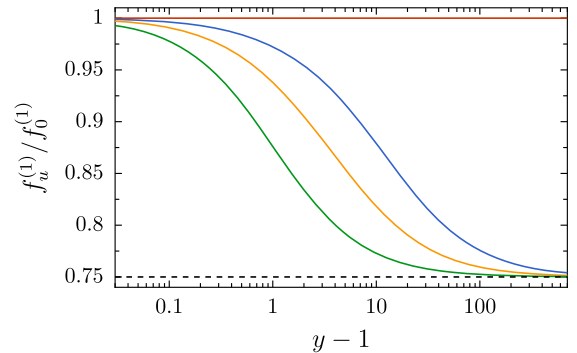

FIG. 3. Ratio $f_u^{(1)}/f_0^{(1)}$ versus $y - 1$ for different values of $u = 0, 0.04, 0.10, 0.25$ from top to bottom. All curves for $u \neq 0$ go from the value 1 at $y - 1 \ll 1$ (top line, $u = 0$) to the value $3/4$ at $y - 1 \gg 1$ (bottom dashed line).
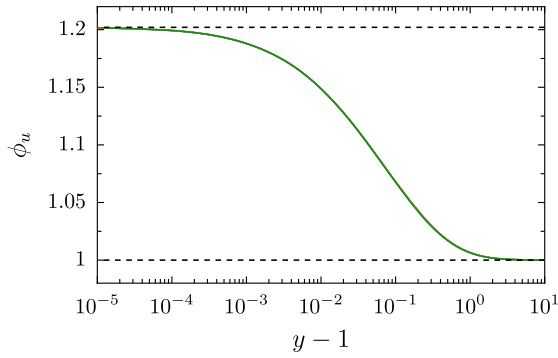
FIG. 4. Ratio $\phi_u \equiv f_u/f_u^{(1)}$ with the same conventions as on Fig. 2, except that a linear scale is used for the ordinate. The curves for different values of u are practically indistinguishable from each other. They produce a universal function decreasing from $\zeta(3) \simeq 1.202$ at small $y - 1$ (top dashed line) to 1 at large $y - 1$ (bottom dashed line).

configurations are identical except for the sign. We stress that such coincidence does not hold for the intermediate distances relevant for applications.

A remarkable fact appears when drawing the ratio of the full expression f_u to the single round-trip expression $f_u^{(1)}$:

$$\phi_u(y) \equiv \frac{f_u(y)}{f_u^{(1)}(y)}. \tag{13}$$

As expected from previous discussions, this ratio goes from the constant $\zeta(3) \simeq 1.202$ at small values of $y - 1$ to the constant 1 at large values of $y - 1$. We see in Fig. 4 the even stronger property that the ratio ϕ_u is a monotonically decreasing function of $y - 1$ depending very weakly on the parameter u. Precisely, the curves drawn on Fig. 4 with the same conventions as on Fig. 2 are practically indistinguishable from each other, which corresponds to a nearly exact conformal invariance. The very weak dependence on u is assessed by calculating numerically the ratio $\phi_u/\phi_\star$ with $\phi_\star$ evaluated for a fixed value $u = u_\star$. Choosing for $u_\star$ the value $u = 0.1$ minimizes the deviation of $|\phi_u/\phi_\star - 1|$, which remains smaller than 4×10^{-4} on the whole domain of parameters $y > 1$ and $0 \leq u \leq 1/4$.

The reason for this nice universality property can be understood qualitatively. The contributions of multiple round-trips are important when the single round-trip contributions are themselves large, that is in the domain $y - 1 \ll 1$ where all contributions tend to become independent of u. A significant dependence of contributions on u would appear in the opposite domain, but ϕ_u is anyway close to unity there since f_u and $f_u^{(1)}$ tend to become identical. These simple arguments explain why the dependence of ϕ_u on u remains weak.

It is furthermore possible to find a rational function of the argument e^{y-1} which fits the different curves ϕ_u with a small maximal error on the whole domain of parameters:

TABLE I. Table of coefficients to be used in the model (15) for $n = 2$ with maximal deviation $\epsilon = 1.2 \times 10^{-3}$.

	$k = 1$	$k = n = 2$
ν_k	0.004 618	0.096 39
μ_k	0.004 415	0.083 97

$$\left| \frac{\phi_u(y)}{\phi_{\mathrm{RM}}(y)} - 1 \right| < \epsilon. \tag{14}$$

The rational model function ϕ_{RM} has the following form:

$$\phi_{\mathrm{RM}}(y) = \prod_{k=1}^{n} \frac{e^{y-1} - 1 + \nu_k}{e^{y-1} - 1 + \mu_k}, \tag{15}$$

where ν_k, μ_k are roots of the polynomials in the numerator and denominator. They have been written as values close to 0, with all values ν_k, μ_k being positive to avoid large deviations on the domain $y > 1$. Inserting the coefficients given in Table I in the rational function (15) leads to a maximal deviation $\epsilon \simeq 1.2 \times 10^{-3}$.

We are left in the end of this reasoning with a largely simplified expression of the full function $f_u(y)$:

$$f_u(y) = f_u^{(1)}(y)\phi_{\mathrm{RM}}(y). \tag{16}$$

The first factor is the analytical single round-trip expression (9) depending on y and u, while the second factor ϕ_{RM} is the rational function (15) with the associated parameters given in Table I. This leads to an accuracy which should be sufficient for most applications [32].

As already mentioned, analogous universality properties were discussed for the Casimir free energy between metallic spheres in vacuum described by the Drude model at the high-temperature limit [10,11]. There, the reason for the universality was that the dielectric function of the spheres tends to infinity at zero frequency, due to the finite static conductivity of metals. In this sense, the problem studied here is dual of the preceding one, with the medium, salted water, exhibiting a finite static conductivity. For the problem of metallic spheres, the factor $-\ell/(\ell + 1)$ in Eq. (8) has to be replaced by unity [30], thereby changing the details of the results while preserving most qualitative discussions. A significant difference comes from the evaluation of the minimal distance for which the free energy is mainly given by the zero-frequency Matsubara term. In the case of vacuum, this distance is the thermal wavelength 7.6 μm, whereas a much smaller distance $\ell_T \sim 0.1$ μm is found in the case of salted water [33]. The universal expression studied in the present Letter describes the force accurately on a much broader distance range than the analogous expression for metallic spheres in vacuum. Furthermore, there exists a wide range of distances

where the Casimir force is sufficiently strong to make the universal thermal contribution of the electromagnetic field experimentally accessible [16].

In the end, the results of this Letter imply that two spherical objects approaching each other in salted water with strong screening undergo a nonscreened Casimir interaction having a universal dependence on geometric parameters, but no dependence on dielectric properties of the spheres. This interaction should have important potential consequences for the physics of biological interfaces and colloids as soon as it represents a significant fraction of the thermal energy $k_B T$ as the immersion in water imposes a Brownian motion to the spheres. This condition is met when the distance L is of the order of or smaller than one-tenth of the effective radius (see Figs. 1 and 2). In the associated domain $y - 1 \lesssim 0.1$, the interaction is mainly determined by the conformally invariant parameter y characterizing the two-spheres geometry, so that the breaking of exact conformal invariance through a dependence on u remains weak (see Fig. 3). The interaction cannot be deduced precisely from any of the two limiting cases (11) or (12), but its estimation is easily deduced from Eq. (16) with the function ϕ_{RM} having significant variations in the domain of interest for biological interfaces (see Fig. 4).

---

[*] gert.ingold@physik.uni-augsburg.de
[†] pamn@if.ufrj.br
[‡] serge.reynaud@lkb.upmc.fr

[1] H. B. G. Casimir, On the attraction between two perfectly conducting plates, Proc. K. Ned. Akad. Wet. **51**, 793 (1948).

[2] R. Decca, V. Aksyuk, and D. López, Casimir force in micro and nano electro mechanical systems, in *Casimir Physics*, edited by D. Dalvit, P. Milonni, D. Roberts, and F. da Rosa, Lecture Notes in Physics, Vol. 834 (Springer, New York, 2011), Chap. 9, p. 287.

[3] T. Gong, M. R. Corrado, A. R. Mahbub, C. Shelden, and J. N. Munday, Recent progress in engineering the Casimir effect – applications to nanophotonics, nanomechanics, and chemistry, Nanophotonics **10**, 523 (2021).

[4] M. E. Fisher and P.-G. de Gennes, Wall phenomena in a critical binary mixture, C. R. Acad. Sci. Paris B **287**, 207 (1978).

[5] T. W. Burkhardt and E. Eisenriegler, Casimir Interaction of Spheres in a Fluid at the Critical Point, Phys. Rev. Lett. **74**, 3189 (1995).

[6] A. Hanke, F. Schlesener, E. Eisenriegler, and S. Dietrich, Critical Casimir Forces between Spherical Particles in Fluids, Phys. Rev. Lett. **81**, 1885 (1998).

[7] C. Hertlein, L. Helden, A. Gambassi, S. Dietrich, and C. Bechinger, Direct measurement of critical Casimir forces, Nature (London) **451**, 172 (2008).

[8] A. Magazzù, A. Callegari, J. Pablo Staforelli, A. Gambassi, S. Dietrich, and G. Volpe, Controlling the dynamics of colloidal particles by critical Casimir forces, Soft Matter **15**, 2152 (2019).

[9] V. A. Parsegian, *Van der Waals Forces* (Cambridge University Press, Cambridge, England, 2006).

[10] A. Canaguier-Durand, G.-L. Ingold, M.-T. Jaekel, A. Lambrecht, P. A. Maia Neto, and S. Reynaud, Classical Casimir interaction in the plane-sphere geometry, Phys. Rev. A **85**, 052501 (2012).

[11] G. Bimonte and T. Emig, Exact Results for Classical Casimir Interactions: Dirichlet and Drude Model in the Sphere-Sphere and Sphere-Plane Geometry, Phys. Rev. Lett. **109**, 160403 (2012).

[12] M. Boström and B. E. Sernelius, Thermal Effects on the Casimir Force in the 0.1–5 μm Range, Phys. Rev. Lett. **84**, 4757 (2000).

[13] A. O. Sushkov, W. J. Kim, D. A. R. Dalvit, and S. K. Lamoreaux, Observation of the thermal Casimir force, Nat. Phys. **7**, 230 (2011).

[14] V. Parsegian and B. Ninham, Toward the correct calculation of van der Waals interactions between lyophobic colloids in an aqueous medium, J. Colloid Interface Sci. **37**, 332 (1971).

[15] P. A. Maia Neto, F. S. S. Rosa, L. B. Pires, A. B. Moraes, A. Canaguier-Durand, R. Guérout, A. Lambrecht, and S. Reynaud, Scattering theory of the screened Casimir interaction in electrolytes, Eur. Phys. J. D **73**, 178 (2019).

[16] L. B. Pires, D. S. Ether, B. Spreng, G. R. S. Araújo, R. S. Decca, R. S. Dutra, M. Borges, F. S. S. Rosa, G.-L. Ingold, M. J. B. Moura, S. Frases, B. Pontes, H. M. Nussenzveig, S. Reynaud, N. B. Viana, and P. A. Maia Neto, Probing the screening of the Casimir interaction with optical tweezers, Phys. Rev. Research **3**, 033037 (2021).

[17] D. S. Ether, Jr., L. B. Pires, S. Umrath, D. Martinez, Y. Ayala, B. Pontes, G. R. d. S. Araújo, S. Frases, G.-L. Ingold, F. S. S. Rosa, N. B. Viana, H. M. Nussenzveig, and P. A. Maia Neto, Probing the Casimir force with optical tweezers, Europhys. Lett. **112**, 44001 (2015).

[18] A. Lambrecht, P. A. M. Neto, and S. Reynaud, The Casimir effect within scattering theory, New J. Phys. **8**, 243 (2006).

[19] B. Spreng, P. A. Maia Neto, and G.-L. Ingold, Plane-wave approach to the exact van der Waals interaction between colloid particles, J. Chem. Phys. **153**, 024115 (2020).

[20] J. N. Israelachvili, *Intermolecular and Surfaces Forces*, 3rd ed. (Academic Press, New York, 2011).

[21] D. J. Mitchell and P. Richmond, A general formalism for the calculation of free energies of inhomogeneous dielectric and electrolytic system, J. Colloid Interface Sci. **46**, 118 (1974).

[22] J. Mahanty and B. W. Ninham, *Dispersion Forces* (Academic Press, New York, 1976), Vol. 1.

[23] R. O. Nunes, B. Spreng, R. de Melo e Souza, G.-L. Ingold, P. A. Maia Neto, and F. S. S. Rosa, The Casimir interaction

between spheres immersed in electrolytes, Universe **7**, 156 (2021).

[24] J. Schwinger, L. L. DeRaad, and K. A. Milton, Casimir effect in dielectrics, Ann. Phys. (N.Y.) **115**, 1 (1978).

[25] T. J. I. Bromwich, Conformal space transformations, Proc. London Math. Soc. **s1-33**, 185 (1900).

[26] W. Thomson, On the mutual attraction or repulsion between two electrified spherical conductors, Lond. Edinburgh Dublin Philos. Mag. J. Sci. **5**, 287 (1853).

[27] J. C. Maxwell, *A Treatise on Electricity and Magnetism* (Oxford University Press, Oxford, 1873) (reprinted by Dover Publications, New York, 1954).

[28] M. Nieto-Vesperinas, *Scattering and Diffraction in Physical Optics*, 2nd ed. (World Scientific, Singapore, 2006).

[29] B. Spreng, M. Hartmann, V. Henning, P. A. Maia Neto, and G.-L. Ingold, Proximity force approximation and specular reflection: Application of the WKB limit of Mie scattering to the Casimir effect, Phys. Rev. A **97**, 062504 (2018).

[30] T. Schoger and G.-L. Ingold, Classical Casimir free energy for two Drude spheres of arbitrary radii: A plane-wave approach, SciPost Phys. Core **4**, 11 (2021).

[31] E. M. Lifshitz, The theory of molecular attractive forces between solids, Sov. Phys. JETP **2**, 73 (1956).

[32] Should a better accuracy be needed, a lower ϵ could be obtained with a higher order n in the model (15). For example, $n = 4$ leads to a maximal error matching the level of deviations between different curves ϕ_u.

[33] The nonzero Matsubara terms can be evaluated by using the results in Ref. [19]; ℓ_T depends on the ratios of dielectric functions of spheres and water at nonzero Matsubara frequencies. The number given in the text is a maximum value for cases studied in Refs. [14–16].